MAIT Journal of Science & Technology
Issue No. 1, Volume No. 2, December 2025, Page No. 27-36
ISSN(Online)

Dynamic Distribution Locational Marginal Pricing Strategy from Electric Vehicles

Vansh Suri[1], Neelu Nagpal[2], Ravi Sharma[1]

[1]Department of Electrical Engineering, MAIT, New Delhi, India
[2]Department of Electronics & Communication Engineering, MAIT, New Delhi, India

Dynamic Distribution Locational Marginal Pricing Strategy from Electric Vehicles

Vansh Suri[1], Neelu Nagpal[2], Ravi Sharma[1]

[1]Department of Electrical Engineering, MAIT, New Delhi, India
[2]Department of Electronics & Communication Engineering, MAIT, New Delhi, India

Abstract

This paper presents a single Quadratic Unconstrained Binary Optimization (QUBO) model of the combined optimization of both active and reactive power dispatch of an Electric Vehicle Aggregator (EVA). Its methodology integrates a new tri-layered, nested optimization framework that streamlines the process of selecting an optimum timetable of the EVA, checking its feasibility with grid limits at the Distribution System Operator (DSO) tier, and then distributing the ultimate schedule to each EV. The resulting framework results in a multi-level, comprehensive evaluation of the system, which generates (a) economically optimal results of both the EVA and the DSO, (b) detailed active and reactive power schedules on the cluster level of the electric vehicles, and (c) in-depth verification of the grid stability in the form of the voltage profiles, power factor, and system losses. Comparative studies indicate that this technique is easily better than benchmark techniques, and results in the reduction of up to 70.5% in total system cost and 29% in active power losses. The findings prove that the suggested QUBO framework can be effectively used as a strong, economically beneficial, and scalable approach to the problem of the demand management of electric vehicles in modern power systems.

Keywords: Demand Response, Electric Vehicle Aggregator, Locational Marginal Pricing, Quadratic Unconstrained Binary Optimization

1. INTRODUCTION

DLMP is a market-based mechanism to determine dynamic location-specific prices based on energy delivery marginal costs (i.e., network congestion losses), which provide the economic signals needed to manage resources efficiently ensure grid reliability [1, 2]. At the distribution level, the DSO first determines an EVA's operational boundaries (i.e., collective battery capacity charging constraints) to leverage distribution-level services [3]. Using dynamic DLMP pricing guidance, the aggregator can then intelligently schedule charging during low-price periods provide vehicle-to-grid (V2G) services during high-price events [4]. Thus, EVs are transformed from passive loads into active, dispatchable assets that can reduce local congestion enhance system resilience. For example, the work of Canizes et al. demonstrated this by using DLMP as a dynamic pricing tool to quantify how much EV users would voluntarily adjust their charging behavior in order to reduce their costs and those of the grid operator [5].

In addition, electric vehicles offer more than just management of active power. With advanced chargers containing voltage source converters, EVs can also supply or absorb reactive power [6]. This means that EVs can provide reactive power even while absorbing zero active power; thus, they have significant potential to provide localized voltage support participate in ancillary service markets [7]. The problem of DLMP-directed reactive demand response from EVAs is a large area of research; studies have utilized various techniques to optimize the DSO–EVA interaction. Traditional modeling approaches typically rely on bilevel programming [10] and hierarchical programming [9]. These bilevel problems have been converted to single-level formulations using the KKT conditions and the strong duality theorem [8, 9, 11]. Other models have utilized quadratic programming [12], Bender's decomposition to solve a Mixed-Integer Nonlinear Program (MINLP) that co-optimizes network reconfiguration with EV user behavior simulation [5], or nonlinear optimization to solve for system-wide social welfare [13]. While these classical optimization methods are well-established, their limitations in handling increasingly complex, discrete, and stochastic environments motivate the exploration of novel computational paradigms. Alongside these established MINLP methods, another class of optimization models, known as binary optimization, has gained prominence in various fields. Among these, QUBO is particularly versatile, with demonstrated success in diverse domains such as finance, cryptography. The primary method for mapping constrained optimization problems, like those found in power systems, into the QUBO format is the use of penalty techniques—a process that involves integrating the problem's constraints directly into the objective function as penalty terms [16, 17].

Although its underlying importance has been recognized, the current literature reveals numerous gaps in research that underpin the need to conduct the inquiry. First of all, the popularity of classical optimization methods can be mentioned. When used on multi-level problems, such techniques typically involve a significant computational cost and, in contrast to other computational frameworks, they do not guarantee global optimality, making it challenging to explore alternative frameworks with potentially faster and stronger convergence properties[18]. In order to address these deficiencies, the current study proposes a new approach with a unique optimization design and less biased performance criteria. The key element of the suggested solution is the unified Quadratic Unconstrained Binary Optimization (QUBO) framework that involves two salient methodological developments. It initially reverses the traditional optimization path by initially setting up an upper-level problem posed in the EV Aggregator (EVA) viewpoint, thus arriving at an optimum power plan via consideration of the existing day-ahead locational marginal prices (DLMPs). Secondly, it replaces classical Karush-Kuhn-Tucker (KKT) duality transforms with a specific QUBO model to break down the nested tri-level optimization problem of coordinated power flow among EV clusters. This detailed information of the methodology is outlined in Section 2.

The main contributions of this study, stemming from these methodological and analytical innovations, are summarized as follows.

- Formulation of the DLMP-driven optimization problem as a QUBO model, with penalty factors derived from Lagrangian Multipliers.
- A rigorous evaluation designed to isolate and quantify the benefits of dedicated reactive power (Qeva-only) support from EVAs for improving grid voltage stability and system efficiency.
- A comprehensive performance evaluation across scenarios designed to test the adaptability of the proposed framework under diverse operational conditions.
- A novel directional power flow visualization that provides an intuitive blueprint of network loading and stress resulting from EV placement during peak hours.
- Benchmarking of the proposed framework against a state-of-the-art method to demonstrate significant improvements in economic efficiency, system performance, and grid stability.

2. PROPOSED METHODOLOGY

In the proposed framework as shown in Figure 1, an EVA optimization at the first level and a DSO optimization at the second level are coordinated through DLMPs. The DLMPs for active and reactive power in each bus and time slot, denoted as $\lambda_{i,t}^{P}$&$\lambda_{i,t}^{Q}$ sensitive price signals reflecting the marginal cost of power delivery. Binary encoding of power variables is achieved, and the resulting output includes cluster-level optimal active and reactive power schedules $P_{c,i,t}^{eva}$ & $Q_{c,i,t}^{eva}$ across time and location. In the second stage, the DSO receives the aggregated active and reactive power schedule from the EVA's optimization and solves its own QUBO problem. The DSO's objective is to minimize the total cost of grid operation, which includes dispatch from distributed generators (DGs), renewable energy sources (PV and wind), and power drawn from the transmission-distribution (TD) interface. All DSO operational constraints—including active and reactive power balance, voltage limits, TD interface power factor, and generator limits—are encoded as penalty terms within the objective function of QUBO. In case the DSO confirms feasibility, the final stage involves EVA Individual Load Allocation, where the aggregated cluster schedule is distributed across individual EVs attached to the specific buses in the system. This is handled through another QUBO optimization, with the corresponding objective. The allocation seeks to minimize reference tracking error and intra-cluster charging interruption cost, subject to constraints including cluster-level tracking, charging smoothness, individual EV energy satisfaction, and rated power limits. The output of this step is the individual EV-level power schedule, specifies how much power each EV should draw at each time slot.

3. OPTIMIZATION FRAMEWORK

A standard QUBO problem is represented by the following function:

$$\min_{\eta} H(J,h) = \sum_{i,j} J_{i,j}\eta_i\eta_j + \sum_i h_i\eta_i \tag{1}$$

where $\eta \in \{0,1\}^N$ is a vector of N binary decision variables, J is a symmetric matrix representing the quadratic interaction weights between variables, and h is a vector of linear biases [15].

The hierarchical framework is discussed in the following subsections.

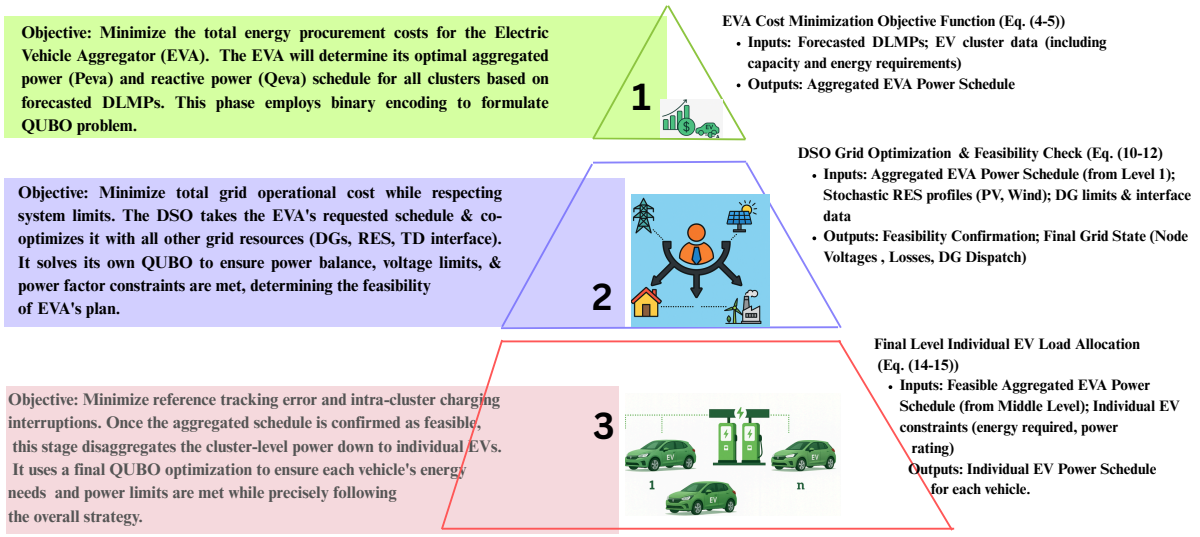

Figure 1: Proposed Hierarchical Optimization Methodology.

3.1 EVA Optimization Problem (Upper-Level)

Minimization of objective function, O_{eva} is subject to a set of constraints that represent the physical and operational limits of the EV fleet, including the instantaneous power limits, total energy requirements for each cluster, the apparent power capacity of the chargers, and the allowable range for reactive power injection or absorption.

$$\min_{P,Q} \quad O_{\text{eva}} = \sum_{c\in C}\sum_{i\in I}\sum_{t\in T}\left(P^{\text{eva}}_{c,i,t}\cdot\lambda^{P}_{i,t} + Q^{\text{eva}}_{c,i,t}\cdot\lambda^{Q}_{i,t}\right) \tag{2}$$

subject to constraints:

$$\left.\begin{aligned}
&\underline{P}_c \le P^{\text{eva}}_{c,t} \le \bar{P}_c, && \forall c,t\\
&\underline{E}_c \le \textstyle\sum_t P^{\text{eva}}_{c,t} \le \bar{E}_c, && \forall c\\
&\left(P^{\text{eva}}_{c,t}\right)^2 + \left(Q^{\text{eva}}_{c,t}\right)^2 \le \left(S^{\text{Rated}}_{c,t}\right)^2, && \forall c,t\\
&\underline{Q}^{\text{eva}}_{c,t} \le Q^{\text{eva}}_{c,t} \le \bar{Q}^{\text{eva}}_{c,t}, && \forall c,t
\end{aligned}\right\}$$

To adapt the constrained problem (refer Equation (2)), we must first transform its continuous power variables into a binary format QUBO formulation. This is done by approximating any real-valued variable P as a weighted sum of binary variables x_k:

$$P = \sum_{k=0}^{d-1} x_k \cdot 2^k, \quad \text{where } x_k \in \{0,1\} \tag{3}$$

In this new formulation, the original constraints are embedded within the objective function as quadratic penalty terms, each weighted by a coefficient ρ_j. The resulting unconstrained objective function to be minimized is:

$$\min \quad Z = \underbrace{\sum_{c,i,t,k}\left(x^{P}_{c,i,t,k}\cdot 2^k\cdot\lambda^{P}_{i,t} + x^{Q}_{c,i,t,k}\cdot 2^k\cdot\lambda^{Q}_{i,t}\right)}_{\text{Operational Cost}} + \underbrace{\sum_{j=1}^{7}\rho_j\cdot\text{Penalty}_j}_{\text{Constraint Penalties}} \tag{4}$$

The individual penalty terms, which correspond to the seven original constraints, are defined as follows:

$$\left.\begin{aligned}
&\text{Penalty}_{1,2} = \left(P^{\text{eva}}_{c,t} - \bar{P}_c\right)^2\cdot\Theta\left(P^{\text{eva}}_{c,t} - \bar{P}_c\right) + \left(\underline{P}_c - P^{\text{eva}}_{c,t}\right)^2\cdot\Theta\left(\underline{P}_c - P^{\text{eva}}_{c,t}\right) && \text{for Active Power Bound}\\
&\text{Penalty}3,4 = \left(\textstyle\sum_t P^{\text{eva}}_{c,t} - \bar{E}_c\right)^2\cdot\Theta\left(\sum_t P^{\text{eva}}_{c,t} - \bar{E}_c\right) && \text{for Energy Requirement}\\
&\text{Penalty}_5 = \left((P^{\text{eva}}_{c,t})^2 + (Q^{\text{eva}}_{c,t})^2 - (S^{\text{Rated}}_{c,t})^2\right)^2 && \text{for Apparent Power Limit}\\
&\text{Penalty}_{5,6} = \left(Q^{\text{eva}}_{c,t} - \bar{Q}_c\right)^2\cdot\Theta\left(Q^{\text{eva}}_{c,t} - \bar{Q}_c\right) + \left(\underline{Q}_c - Q^{\text{eva}}_{c,t}\right)^2\cdot\Theta\left(\underline{Q}_c - Q^{\text{eva}}_{c,t}\right) && \text{for Reactive Power Bound}
\end{aligned}\right\} \tag{5}$$

3.2 DSO Optimization Problem (Lower-Level)

$$\min \mathrm{O}_{\mathrm{dso}} = \sum_{t\in T}\left[\sum_{g\in DG}\left(\alpha^{P}_{g,t}P_{g,t}+\alpha^{Q}_{g,t}Q^{\mathrm{abs}}_{g,t}\right)+\sum_{i\in TDg}\left(\Gamma^{TDg}_{i,t}\left(P^{TDfx}_{i,t}-P^{TDg}_{i,t}\right)+L^{TDg}_{i,t}Q^{\mathrm{abs}}_{i,t}\right)\right] \tag{6}$$

subject to constraints:

$$\left.\begin{array}{ll}
\sum_g P_{g,t}+\sum_i P^{TDg}_{i,t}+\sum_i P^{PV}_{i,t}+\sum_i P^{WG}_{i,t}=\sum_j P_{i,j,t}, & \forall i,t\\
\sum_g Q_{g,t}+\sum_i Q^{TDg}_{i,t}-\left(Q^{\mathrm{inflex}}_{i,t}+\sum_c Q^{eva}_{c,i,t}\right)=\sum_j Q_{i,j,t}, & \forall i,t\\
\underline{V}i\le Vi,t\le \bar{V}_i, & \forall i,t\\
\underline{\theta}i\le \theta i,t\le \bar{\theta}_i, & \forall i,t\\
Q^{TD}_{i,j,t}-\tan(\arccos(0.9))\cdot P^{TD}_{i,j,t}\ge 0, & \forall i,j,t
\end{array}\right\}$$

The QUBO formulation of DSO optimization. Here, the objective is to minimize a single function comprising operational costs and penalties for any constraint violations.

$$\min \quad Z=\underbrace{\sum_{g,t,k}\left(x^{P}_{g,t,k}\cdot 2^{k}\cdot\alpha^{P}_{g,t}+x^{Q}_{g,t,k}\cdot 2^{k}\cdot\alpha^{Q}_{g,t}\right)}_{\text{Operational Cost}}+\underbrace{\sum_{j=8}^{13}\rho_j\cdot\mathrm{Penalty}_j}_{\text{Constraint Penalties}} \tag{7}$$

where x are the binary decision variables of the QUBO problem. The various system constraints are embedded into the objective function as quadratic penalty terms. These penalties are defined as follows:

Here, Penalty terms are defined as:

$$\left.\begin{array}{lll}
\mathrm{Penality}_8=\left(\sum_g P_{g,t}+\sum_i P^{TD}_{i,t}+\sum_i P^{PV}_{i,t}+\sum_i P^{WG}_{i,t}-\sum_j P_{D,j,t}\right)^2 & \text{Power Balance Constraint}\\
\mathrm{Penality}_{9,10}=(V_i-\bar{V}i)^2\cdot\Theta(V_i-\bar{V}_i)+(\underline{V}_i-V_i)^2\cdot\Theta(\underline{V}_i-V_i) & \text{Voltage Limit Violation}\\
\mathrm{Penality}_{11}=\left(Q^{TD}_{i,t}-0.484\cdot P^{TD}_{i,t}\right)^2\cdot\Theta(\mathrm{violation}) & \text{TD Interface Power Factor}\\
\mathrm{Penality}_{12,13}=(P_{g,t}-\bar{P}g)^2\cdot\Theta(Pg,t-\bar{P}_g) & \text{Generator Limit Violation}
\end{array}\right\} \tag{8}$$

3.3 EVA Individual EV Load Allocation

$$\min \mathrm{O}_{\mathrm{evla}}=\sum_{t=1}^{T}\sum_{c=1}^{C}\left(\left|\delta^{eva}_{c,t}\right|\cdot\omega_1+\left|\gamma^{\mathrm{intrup}}_{c,t}\right|\cdot\omega_2\right) \tag{9}$$

where, $\delta^{eva}_{c,t}$ is the difference (error) between the scheduled total and $\gamma^{\mathrm{intrup}}_{c,t}$ refers to what was allocated across EVs and total intra-cluster power fluctuation or interruption cost for EVA. The constraints can be given by:

$$\left.\begin{array}{ll}
P^{\mathrm{eva}}_{c,t}-\sum_{n=1}^{N}\hat{P}^{\mathrm{eva}}_{n,t}=\delta^{\mathrm{eva}}_{c,t}, & \forall c,t\\
\sum_{n=1}^{N}\left|\hat{P}^{\mathrm{eva}}_{n,t}-P^{\mathrm{eva}}_{n,t+1}\right|=\gamma^{\mathrm{intrup}}_{c,t}, & \forall c,t\\
\sum_{t=1}^{T}\hat{P}^{\mathrm{eva}}_{n,t}=E^{\mathrm{eva}}_{n}, & \forall n\\
0\le\hat{P}^{\mathrm{eva}}_{n,t}\le P^{\mathrm{rated}}_{n}, & \forall n,t
\end{array}\right\} \tag{10}$$

The QUBO formulation of equation (9) is given below.

$$\min\sum_{t,c}\left(\left|\delta^{eva}_{c,t}\right|\cdot\omega_1+\left|\gamma^{\mathrm{intrup}}_{c,t}\right|\cdot\omega_2\right)+\sum_{j=13}^{15}\rho_j\cdot\mathrm{Penalty}_j \tag{11}$$

At the dispatch level, the Electric Vehicle Aggregator (EVA) uses the following penalty terms to ensure both aggregate and individual EV charging targets are met: The penalty terms for the EVA dispatch level are defined as follows:

$$\left.\begin{array}{lll}
\mathrm{Penalty}_{13}=\left(P^{\mathrm{eva}}_{c,t}-\sum_n\hat{P}^{\mathrm{eva}}_{n,t}\right)^2 & \text{Aggregator Reference Tracking}\\
\mathrm{Penalty}_{14}=\left(\sum_t\hat{P}^{\mathrm{eva}}_{n,t}-E^{\mathrm{eva}}_{n}\right)^2 & \text{Individual EV Charging Fulfillment}\\
\mathrm{Penalty}_{15}=\left(\hat{P}n,t^{eva}-P^{\mathrm{rated}}_{n}\right)^2\cdot\Theta\left(\hat{P}n,t^{eva}-P^{\mathrm{rated}}_{n}\right) & \text{EV Maximum Charging Rate Violation}
\end{array}\right\} \tag{12}$$

where, $P_{c,t}^{\text{eva}}$ is the reference power schedule for the entire aggregator; $\hat{P}_{n,t}^{\text{eva}}$ is the dispatched charging power to an individual EV n at time t; E_n^{eva} is the total energy required by EV n; P_n^{rated} is the maximum rated charging power for EV n.

Table 1: Comprehensive Simulation and Computational Setup.

Parameter	Description	Value
System & Network Model		
System	IEEE standard radial distribution network	33-bus
Time Horizon	Total simulation duration and discretization	24 hours (6 slots × 4h)
Assets & Loads		
EV Population	Number and aggregation of electric vehicles	1000 (20 spectral clusters)
Optimization & Pricing		
Optimization Model	Framework for scheduling active/reactive power	QUBO
QUBO Encoding	Binary variable precision for scheduling	8 bits (primary) + 4 bits (sensitivity)
DLMP Scheme	Pricing for active and reactive power	
Base Case	Fixed hourly prices for active power	λ_P: [40, 50, 60, 70, 100, 60] \$/MWh
	Price range for reactive power	λ_Q: [4–10] \$/MVArh
Computational Environment		
Execution Platform	Primary environment for reported results	Google Colaboratory (Colab)
Runtime Type	Processor used on Colab	*CPU (Standard) / GPU (Tesla T4)**
Development Machine	Local machine for coding and initial tests	Dell G15
CPU / RAM		Intel i5-11260H / 8 GB
GPU	(Part of dev. environment, not core calc.)	NVIDIA GeForce RTX 4060
Software	Core language and key libraries	
Language		Python 3.10
Core Libraries	Numerical, Data, and Network Modeling	NumPy, SciPy, Pandas, NetworkX
Visualization	Plotting and data visualization	Matplotlib, Seaborn
Utility	Progress tracking during optimization	TQDM

4. SIMULATION RESULTS AND DISCUSSION

This section includes the performance evaluation of the optimized structure of the proposed optimization framework for the IEEE 33-Bus System modified with a single 500 kW Photovoltaic (PV) System located at bus 15 and three 500 kW Wind Turbines located at bus 7. The purpose of this simulation study, as shown in Table 1 and described in detail, is to evaluate how well the system can perform under increasingly complex conditions. The research begins with a relatively simple evaluation (Scenarios S_1-S_2), and continues through to add complexity in two stages; first through the introduction of Reactive Power Dispatch (#S_3), and second through the inclusion of Adaptive Pricing (#S_4) into the previous stage of analysis. The ability of the proposed optimization to keep the critical grid parameters within acceptable bounds is demonstrated by the ability to maintain each buses' voltage levels within a standard operating range of 0.95-1.05 p.u. during peak periods (see Figure 2a) thereby providing a stable base upon which to minimize losses. Additionally, the power factor at the T-D interface is maintained constant and close to unity at all times (as shown in Figure 2b). These results indicate the optimization's effectiveness in keeping the critical grid parameters within acceptable limits; this can be seen in Figure 2 for each of the cases studies. To ensure that the primary needs of maintaining acceptable voltage levels at the T-D interface and acceptable current flow through each distribution line are met, secondary performance metrics were evaluated. These include Power Deviation (PD), i.e., the deviation of the total power delivered over a time period from the reference schedule (i.e., the difference between the actual amount of energy delivered during the same time frame

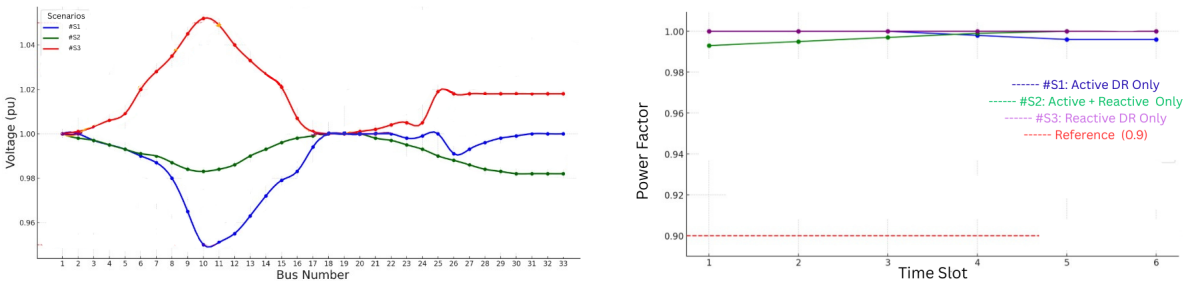

(a) Voltage Profile at Peak Hour.

(b) Power Factor at T-D Interface.

Figure 2: Validation of the proposed optimization approach across different scenarios, showing (a) the bus voltage profiles and (b) the power factor at the T-D interface.

and the scheduled amount of energy); and Line Loading, i.e., the time varying percent of power flow on a given distribution line relative to the lines rated maximum allowable capacity. In addition, the impact of the different scenarios on the characteristics of the system is also explored, specifically the network topology with power flow. This is the representation of the grid's structure, which shows the buses (nodes), lines (edges), and the direction and magnitude of the power flow.

4.1 Performance Analysis of System

This section provides a performance analysis for two scenarios ($\S_1$–$\S_2$) to compare our proposed framework with another approach given in [8].

4.1.1 Scenario $\S_1$: Baseline Case without Demand Response

The results of the simulation in the case of the baseline scenario ($\S_1$), where the EVA receives only active power and demand response (DR) is not carried out, are presented in this section. Figure 3 in the appendix shows that optimization results in a continuously constant active power consumption of 3.3325 MW through the whole day. This constant rate of charge supports the fact that there is no load shifting, as specified in the scenario. This observation is further confirmed by Figure 3a, which shows that all electric vehicle (EV) clusters have a fixed rate of charging over the time horizon. As a result, there are no adaptive charging policies and responsive power control. The charging schedule is fixed and immobile, which brings about severe network inefficiency and stress. The line-loading distribution shown in Figure 3b indicates that the load distribution is highly skewed: most of the lines are lightly loaded, and some of them are heavily overloaded. This kind of arrangement is the sign of the inefficient use of resources and the appearance of bottlenecks due to the stagnant flows of power. In order to explain the cause of such an imbalance, it is instructive to examine the network topology (Figure 3c) alongside the EV demand profiles (Figure 3d). The overall examination elucidates the loci of stress. An example would be a cluster with heavy energy requirement at a distance (a bus) far away to the substation which automatically induces large power flows and power losses which are directly traced in the highly stressed lines that are defined by the histogram.

Further examination of the simulation outcome indicates the operational disadvantages of this method. Figure 3e indicates considerable differences between the actual and reference charging patterns, particularly during the transition phases between off-peak and peak demand (slots 1 and 6). These reference patterns, described by Equation 2, are used as penalty functions in the QUBO objective function. The differences indicate a lack of temporal synchronization in cluster charging, despite the constant total load. At the same time, Figure 3f indicates the total system line losses, which increase over time during peak periods. Since this case does not offer reactive power compensation, the system inherently suffers from higher I^2R losses; without reactive compensation, the system requires greater current injections for grid balance, which is solely addressed by active power dispatch.

*4.1.2 S_2:**With Active and Reactive DR***

In this case, the EVA functions as a prosumer by engaging in both active and reactive DR with substantial improvements over the baseline scenario (S_1). Unlike in the previous scenario, the optimized active power consumption, P^{eva}, is now time-varying and optimally varied over time intervals (Figure 4a), while the EVA also injects reactive power, Q^{eva}, into the grid (Figure 4b). This synchronized control directly enhances the health of the network by ensuring more balanced line loading (Figure 4c) across the topology of the system (Figure 4d) and ensuring voltage stability at the buses, as reflected by the small variations on the heat map (Figure 4e). The main effect of this optimized control is a substantial reduction in total active power losses compared to the baseline (Figure 4f). These system-level benefits are achieved by optimally dispatching individual EV clusters according to their energy demand and availability (Figure 4h), with their individual active and reactive contributions shown in Figure 4i. Another indication of the support role of the EVA is reflected at the T-D interface, where P^{eva} is constant while Q^{eva} reduces during peak hours to offer ancillary services (Figure 4g). Although this optimized control schedule varies from the initial reference given by Equation 2 (Figure 4j), it is this flexibility that makes it possible to achieve substantial improvements in the efficiency and stability of the grid.

Even for the two similar scenarios, the proposed study offers a more comprehensive analysis by considering a broader set of metrics. This includes a thorough analysis of the grid performance (such as line loading histogram analysis, voltage profile analysis), optimization process (such as convergence analysis, bit depth analysis), and model-specific criteria (such as quality of clustering and EVA profitability) as indicated in Table 2 and explained in the next section. The comparative performance analysis of the proposed approach with [8] for the two scenarios, namely S_1 and S_2, is as follows: S_1 is concerned with cost minimization, whereas S_2 also considers reactive support for the grid.

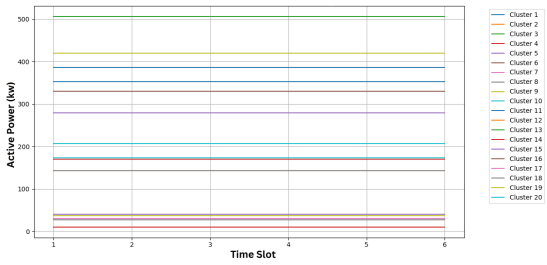

(a) Cluster-wise Charging Profiles

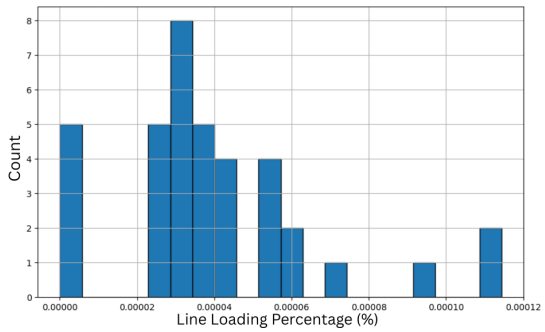

(b) Line Loading Percentage at Peak Hour (Time Slot 5)

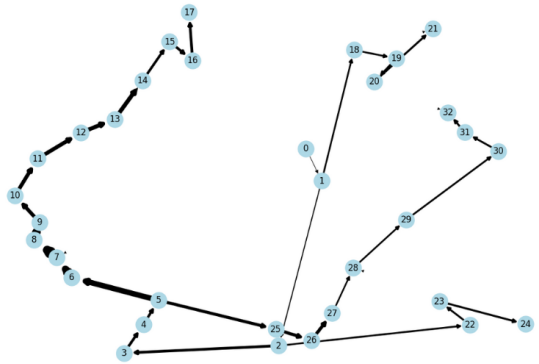

(c) Network Topology with Power Flow at Peak Hour (Time Slot 5)

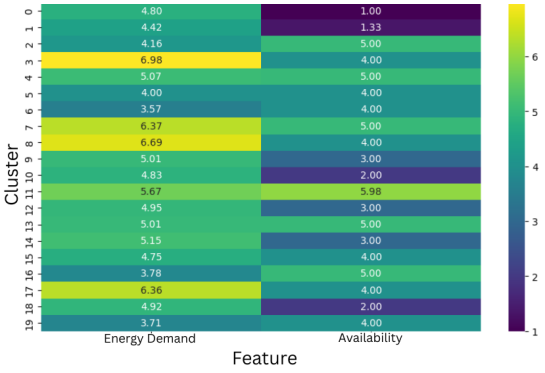

(d) Cluster Distribution Heatmap

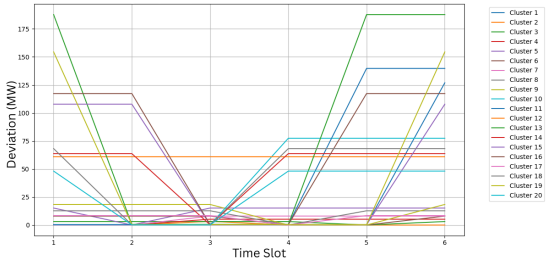

(e) Power Deviation Schedule across Time Slots

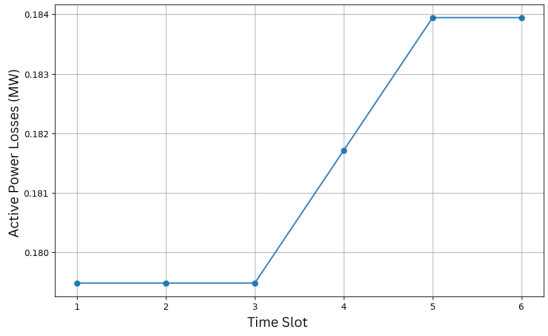

(f) Active Power Losses across Time Slots

Figure 3: System response and grid performance under the conditions of S_1

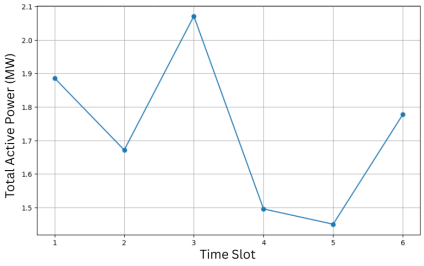

(a) Total Active Power across Time Slots

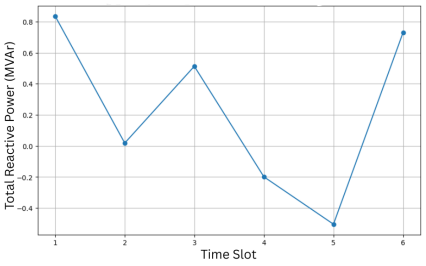

(b) Total Rective Power across Time Slots

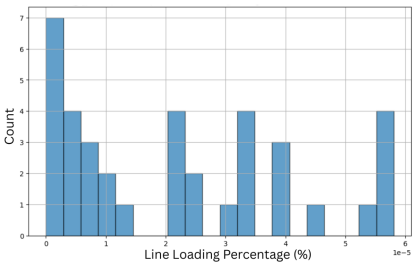

(c) Line Loading Percentage at Peak Hour (Time Slot 5)

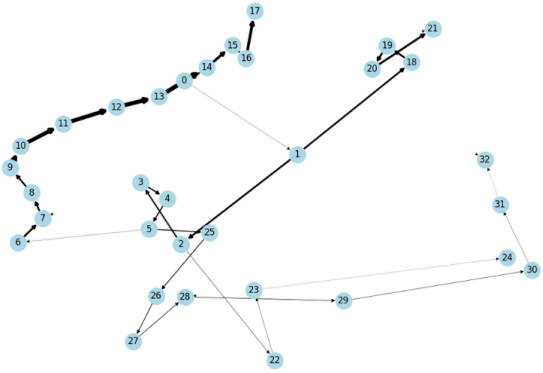

(d) Network Topology with Power Flow at Peak Hour (Time Slot 5)

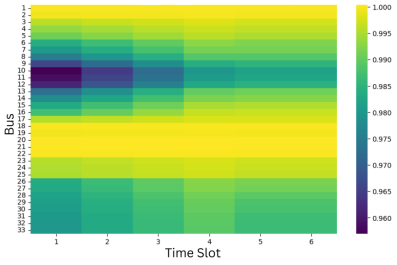

(e) Voltage Heatmap (p.u.)

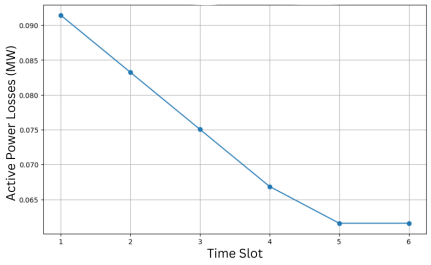

(f) Active Power Losses

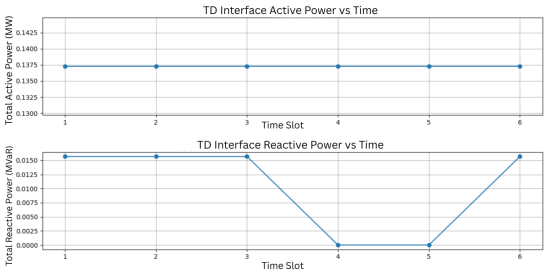

(g) T-D Interface Active and Reactive Powers across Time Slots

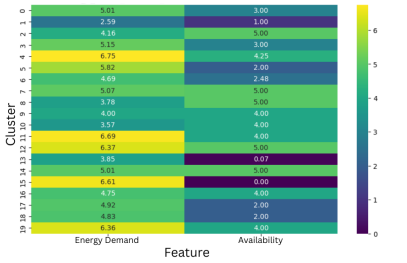

(h) Cluster Distribution Heatmap

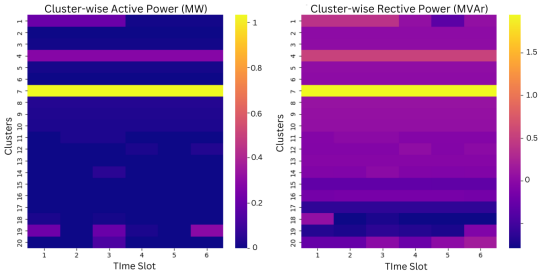

(i) Cluster-wise Active and Reactive Power

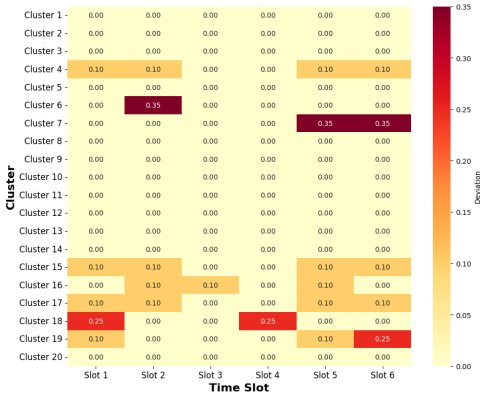

(j) Deviation from Reference Schedule

Figure 4: System response and grid performance under the conditions of $S_2 2$

Table 2: Comparative Performance Analysis of the Proposed Method.

Performance Metric	S_1		S_2		Key Finding / Improvement
	[8]	**Proposed**	**[8]**	**Proposed**	
Methodological Setup					
No. of EVs	1000	1000	1000	1000	Baseline consistency
No. of Clusters	4	20	—	—	QUBO method has Finer granularity.
Clustering Score	0.4010	0.5501	—	—	**37%** Silhouette score
Bit Precision	Cont.	4/8-bit	Cont.	4/8-bit	Enables quantum/digital implementation
Economic Performance					
EVA Cost ($)	1634.80	1132.20	726.31	580.50	**30.7%** (S_1) & **20.1%** (S_2)
DSO Cost ($)	3994.79	526.06	472.20	276.30	**86.8%** (S_1) & **41.5%** (S_2)
Total System Cost ($)	5629.59	1658.26	1198.51	856.80	**70.5%** (S_1) & **28.5%** (S_2)
Reactive Compensation ($)	—	—	15.00	4.95	**67.0%** cost S_2
Grid Technical Performance					
System Active Losses (MWh)	1.75	1.09	0.62	0.44	**37.7%** (S_1) & **29.0%** (S_2)
Minimum Voltage (pu)	N/R	0.9500	0.9501	0.9570	**0.7%** floor in S_2
Avg. Voltage (pu)	∼0.985	0.9890	0.9880	0.9905	Consistently closer to 1.0 pu
Voltage Profile Std Dev (pu)	∼0.012	N/R	∼0.012	0.0079	**34% smoother** voltage profile in S_2
Power Factor (TD Interface)	0.985	0.998	N/R	0.998	to near-unity
Total Reactive Energy (MVArh)	—	—	∼110	136.27	**23.9%** reactive support
Operational Constraints & Runtimes					
Charging Interruptions	N/R	N/R	5	2	**60%** interruptions
Constraint Violations	N/R	66	N/R	75	Comparable constraint adherence
QUBO Runtime (4-bit) (s)	—	69.5	—	—	Fast computation time
QUBO Runtime (8-bit) (s)	—	326.6	—	—	Trade-off for higher precision

N/R: Not Reported; Cont.: Continuous variables; —: Not applicable

4.1.3 Comparison with Reported Work

The performance of the proposed QUBO optimization method is benchmarked against the reported work in [8]. The previous study has considerd two primary cases that correspond to our cost-minimization scenario (S_1) and reactive power support scenario (S_2). Consequently, a direct performance comparison for these two scenarios, with their respective results are summarized in Table 2. As detailed in Table 2, the proposed QUBO framework demonstrates substantial and multifaceted improvements over the benchmark approach. From an economic perspective, the framework drastically reduces costs for both the EVA and the DSO, leading to a remarkable reduction in total system cost - by more than 70% in the baseline scenario (S_1). These financial gains are underpinned by superior grid management, evidenced by significant reductions in active power losses and a markedly improved voltage profile, which is improved and more stable. Methodologically, performance gains are driven by a finer-grained clustering approach and the use of a bit-based optimization model. Operationally, the system achieves these benefits with fewer charging interruptions and computationally viable runtime, confirming the practical applicability of the proposed framework.

5. CONCLUSION

This paper introduced a new integrated three-level QUBO-based optimization model that was designed to address the demand response problem based on the DLMP. A sequential, modular framework offers an alternative to classical bilevel methods, which is both practical and scalable, and which attempts to capture the interaction between the EVA and the DSO in its hierarchical nature under diverse operational conditions. The findings prove the obvious excellence and flexibility of the suggested strategy. A direct comparison with an existing approach demonstrates that our framework is capable of lowering the overall price of the system using active demand response and using both active and reactive demand response, without exceeding the limits of the important parameters of the grid. The work affirms that EV flexibility intelligently operated through dynamic market information is a very crucial and economically viable asset in developing a more robust and stable distribution grid. The future work must be directed at improving the framework and making it more curtailment-reducing-strategy-specific to ensure the economic and environmental performance of such complicated energy systems is improved.

REFERENCES

[1] C. Sabillon, A. A. Mohamed, B. Venkatesh and A. Golriz, "Locational Marginal Pricing for Distribution Networks: Review and Applications," 2019 IEEE Electrical Power and Energy Conference (EPEC), Montreal, Canada, 2019, pp. 1–5.

[2] L. Bai, J. Wang, C. Wang, C. Chen and F. Li, "Distribution Locational Marginal Pricing (DLMP) for Congestion Management and Voltage Support," *IEEE Transactions on Power Systems*, vol. 33, no. 4, pp. 4061–4073, July 2018.

[3] L. Wang, J. Kwon, N. Schulz and Z. Zhou, "Evaluation of Aggregated EV Flexibility With TSO-DSO Coordination," *IEEE Transactions on Sustainable Energy*, vol. 13, no. 4, pp. 2304–2315, Oct. 2022.

[4] *E-Mobility in Electrical Energy Systems for Sustainability*, Advances in Mechatronics and Mechanical Engineering (AMME), 2024.

[5] B. Canizes, J. Soares, Z. Vale, and J. M. Corchado, "Optimal Distribution Grid Operation Using DLMP-Based Pricing for Electric Vehicle Charging Infrastructure in a Smart City," *Energies*, vol. 12, no. 4, p. 686, 2019.

[6] J. Singh and R. Tiwari, "Electric vehicles reactive power management and reconfiguration of distribution system to minimise losses," *IET Gener. Transm. Distrib., vol. 14, pp. 6285-6293, 2020. https://doi.org/10.1049/iet-gtd.2020.0375

[7] J. Wang, G. R. Bharati, S. Paudyal, O. Ceylan, B. P. Bhattarai and K. S. Myers, "Coordinated Electric Vehicle Charging With Reactive Power Support to Distribution Grids," in IEEE Transactions on Industrial Informatics, vol. 15, no. 1, pp. 54-63, Jan. 2019, doi: 10.1109/TII.2018.2829710.

[8] B. Jangid, P. Mathuria, and V. Gupta, "Distribution Locational Marginal Price Driven Reactive Demand Response from Electric Vehicle Aggregator," *IEEE Transactions on Industry Applications*, vol. 60, no. 4, pp. 5510–5521, 2024. https://doi.org/10.1109/tia.2024.3392884

[9] B. S. K. Patnam and N. M. Pindoriya, "DLMP Calculation and Congestion Minimization With EV Aggregator Loading in a Distribution Network Using Bilevel Program," *IEEE Systems Journal*, vol. 15, no. 2, pp. 1835–1846, 2021. doi:10.1109/JSYST.2020.2997189.

[10] B. Jangid, P. Mathuria and V. Gupta, "Reactive DLMP for Hierarchical Energy Management and Optimal Reactive Power Response from EVs," 2022 22nd National Power Systems Conference (NPSC), New Delhi, India, 2022, pp. 278-283, doi: 10.1109/NPSC57038.2022.10069172.

[11] W. Liu and F. Wen, "Discussion on 'Distribution Locational Marginal Pricing for Optimal Electric Vehicle Charging Management'," *IEEE Transactions on Power Systems*, vol. 29, no. 4, p. 1866, 2014. doi:10.1109/TPWRS.2014.2325414.

[12] Q. Wu, F. Shen, Z. Liu, W. Jiao, and M. Zhang, "Distribution locational marginal pricing for congestion management in distribution networks," in: *Book Chapter*, Elsevier, 2024, pp. 13–28. doi:10.1016/b978-0-443-19015-5.00005-6.

[13] R. Li, Q. Wu, and S. S. Oren, "Distribution Locational Marginal Pricing for Optimal Electric Vehicle Charging Management," *IEEE Transactions on Power Systems*, vol. 29, no. 1, pp. 203–211, 2014. doi:10.1109/TPWRS.2013.2278952.

[14] H. Song, G.-S. Seo, and D.-J. Won, "Pricing Strategy of Electric Vehicle Aggregators Based on Locational Marginal Price to Minimize Photovoltaic (PV) Curtailment," *IEEE Access, vol. 2025, pp. 1–1, 2025. doi:10.1109/access.2025.3528626.

[15] M. Isopi, B. Scoppola, and A. Troiani, "On some features of Quadratic Unconstrained Binary Optimization with random coefficients," Feb. 2024, doi: 10.48550/arxiv.2402.17059.

[16] O. Pichugina, Y. K. Tan, and C. W. Beck, "Deriving Compact QUBO Models via Multilevel Constraint Transformation," Apr. 2024, doi: 10.48550/arxiv.2404.03610. Available: https://arxiv.org/pdf/2404.03610

[17] T. Komiyama and T. Suzuki, "QUBO formulation using inequalities for problems with complex constraints," pp. 55–61, Jan. 2024, doi: 10.1145/3635035.3635042

[18] V. C. Pandey, T. Rawat, J. Ospina, Y. Dvorkin, and C. Konstantinou, "A tri-level distribution locational marginal price-based demand response framework," *Electric Power Systems Research, vol. 241, 2025, 111398. https://doi.org/10.1016/j.epsr.2024.111398.